Resonant Particle Heating of an Electron Plasma by Oscillating Sheaths

B. P. Cluggish,* J. R. Danielson, and C. F. Driscoll
Department of Physics, 0319, University of California at San Diego, La Jolla, California 92093
(Received 27 January 1998)

The first unambiguous measurements of a bounce-resonance effect in a non-neutral plasma are presented. Two striking signatures are observed when a magnetized electron column is heated by oscillating an end sheath. First, the heating rate increases by a factor of 10^4 as the oscillation frequency is increased by a factor of 10 near the thermal electron bounce frequency. Second, the heating is enhanced when the sheaths at both ends are oscillated out of phase, but is suppressed when they are in phase. The measured rates are in quantitative agreement with a resonant particle heating theory. [S0031-9007(98)06580-6]

PACS numbers: 52.25.Wz, 52.20.Dq, 52.50.Gj

Resonant interactions between particles and fields are of broad interest in plasma physics. Landau damping [1] of plasma waves occurs in nearly all plasmas, by particles whose velocities are resonant with the phase velocity of the wave [2], or whose bounce frequencies are resonant with the wave frequency [3]. Magnetic mirror plasmas [4] and some plasma processing discharges [5] are heated by oscillating fields which are resonant with the bounce motions of the electrons. In the magnetosphere, bounce resonances of trapped particles may excite magnetohydrodynamic waves [6] or lead to particle diffusion [7]. In Penning traps, oscillating voltages resonant with the guiding center motions of the trapped particles are used to improve particle confinement [8]. Resonance between guiding center motions and static field asymmetries has long been thought to limit the confinement times in magnetic mirror [9] and non-neutral plasma traps [10], but no clear experimental signature has been found.

Here, we present the first unambiguous measurements of a bounce resonance effect in a non-neutral plasma. A magnetized electron column is heated through resonant interaction between axially bouncing electrons and an oscillating end sheath driven by an oscillating voltage. The measured heating rates are orders of magnitude larger than those due to "adiabatic" oscillation of the end sheaths [11]. The resonant heating has two striking signatures. First, the heating rate increases by a factor of 10^4 as the oscillation frequency is increased by a factor of 10 near the thermal electron bounce frequency. Second, if the same voltage is used to oscillate the sheaths at both ends of the plasma simultaneously, the heating is enhanced when the sheaths oscillate out of phase, but the heating is suppressed when they are in phase.

The measured rates are in quantitative agreement with a resonant particle theory by Crooks and O'Neil [12]. The theory starts from the Fermi acceleration model [13] of particles bouncing between a fixed and a moving wall. Resonant particles undergo large excursions in velocity space due to coherent "kicks" from the moving wall. Interelectron collisions knock the electrons in and out of resonance, causing irreversible heating. This velocity-space transport is analogous to neoclassical configuration-space transport which occurs in fusion plasmas [14].

We confine the electron plasmas in a cylindrical Penning-Malmberg trap [11], shown schematically in Fig. 1. Electrons emitted from a tungsten filament are confined in a series of conducting cylinders of radius $R_w = 1.27$ cm enclosed in a vacuum can at 4.2 K. Background pressure is measured to be $P \lesssim 10^{-11}$ torr. The electrons are confined axially by applying $V_c = -200$ V on cylinders 1 and 5; radial confinement is provided by a uniform axial magnetic field $B = 20$ kG. The trapped electron plasma typically has initial density $10^9 \leq n \leq 10^{10}$ cm^{-3}, radius $R_p \approx 0.06$ cm, and a characteristic radial expansion time $\tau_m \approx 100$–1000 sec. The apparatus is operated in an inject/manipulate/dump cycle, and has a shot-to-shot reproducibility of $\delta n/n \sim 1\%$.

The z-integrated density of the plasma is measured by dumping the electrons onto the end collectors, by grounding cylinder 5. A histogram of the z-integrated density, $Q(r)$, is obtained directly from the charge on the five collectors.

The parallel plasma temperature, $T_\parallel$, is measured by slowly ramping the voltage on cylinder 5 to ground, and measuring the number of electrons which escape as a function of the confining voltage. Four shots are averaged, giving $T_\parallel$ with a precision of about 10%. In the experiments described in this paper, typical temperatures

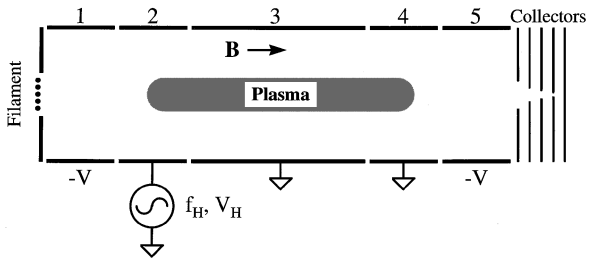

FIG. 1. Schematic of the cylindrical apparatus and electron plasma. Cylinders 2 and 4 are the same length.

are $0.2 \leq T_\parallel \leq 20$ eV, which gives $T_\parallel$ to $T_\perp$ collisional equilibration rates [11] $\nu_{\perp\parallel} \equiv (8/15)\sqrt{\pi}\, nb^2 \overline{v} \ln(r_c/b)$ in the range $10^3 \leq \nu_{\perp\parallel} \leq 10^5$ sec^{-1}, and thermal speeds in the range $2 \times 10^7 \leq \overline{v} \equiv \sqrt{T_\parallel/m} \leq 2 \times 10^8$ cm/s.

We calculate the z-dependent plasma density $n(r, z)$ and space charge potential $\phi(r, z)$ from the measured z-integrated charge $Q(r)$ and $T_\parallel$, by numerically solving Poisson's equation, assuming that the electrons are in local thermal equilibrium along each field line. That is, we assume

$$n(r, z) = n_0(r) \exp\{e\phi(r, z)/T_\parallel\},$$

where $n_0(r)$ is obtained by requiring that $\int n(r, z)\, dz = Q(r)$. The density and potential inside the plasma are nearly uniform in z, but both decrease abruptly in end sheaths of characteristic thickness $\lambda_D \approx 0.01$ cm. Typical plasma lengths are $3 < L_p < 5$ cm. The individual electrons bounce back and forth axially between the plasma ends. The bounce frequency for a thermal electron is typically $2 \leq \overline{f_b} \equiv \overline{v}/2L_p \leq 30$ MHz, such that $\overline{f_b} \gg \nu_{\perp\parallel}$.

We heat the plasma by applying a sinusoidally oscillating voltage V_h to cylinder 2, causing the end sheath to oscillate in z. The amplitude of the applied heating voltage is typically $0.5 \leq V_h \leq 10$ V, and the frequency ranges from $0.1 \leq f_h \leq 20$ MHz. After heating the plasma, we wait several equilibration times $\nu_{\perp\parallel}^{-1}$ before measuring the temperature, to allow the electrons to reach a local thermal equilibrium with $T_\parallel = T_\perp = T$. The heating rate dT/dt is found by measuring the time dt required for the plasma temperature to rise by $dT \approx 0.1T$; typically $1\ \mu\text{sec} \leq dt \leq 40$ ms.

Previous studies [11] measured heating in the *adiabatic* regime of $f_h \ll \overline{f_b}$. Here, the applied voltage causes L_p and $T_\parallel$ to oscillate in phase with the voltage, resulting in irreversible heating due to the collisional relaxation between $T_\perp$ and $T_\parallel$. This adiabatic heating occurs at a rate given by

$$\frac{dT^{\text{abd}}}{dt} = \frac{4}{3}\,\nu_{\perp\parallel} T \left(\frac{\delta L}{L_p}\right)^2 \left[\frac{f_h^2}{f_h^2 + 9\nu_{\perp\parallel}^2/4\pi^2}\right], \quad (1)$$

where $\delta L \propto V_h$ is the amplitude of the oscillation in the plasma length. Note that if $f_h \gg \nu_{\perp\parallel}$, then the heating rate is expected to be independent of f_h. This is observed experimentally, as shown by the $f_h < 1$ MHz data in Fig. 2. The dashed line shows Eq. (1) with $\delta L/L_p = 0.0042$. Here, $\nu_{\perp\parallel} = 45\,000$ sec^{-1} and $\overline{f_b} = 4.8$ MHz.

Resonant particle heating causes dT/dt in Fig. 2 to increase by over 4 orders of magnitude for $f_h > 1$ MHz. That is, energy is given to those electrons with bounce frequencies $f_b = f_h/\ell$, with $\ell = 1, 2, 3, \ldots$. This can be verified experimentally by applying an oscillating voltage to both cylinders 2 and 4 (both cylinders are the same length), so that the sheaths at both ends of the plasma oscillate in z. We use the same f_h and V_h on both cylinders, but phase shift the voltage on one cylinder an amount θ_h with respect to the other. When the voltages on the two cylinders are in phase ($\theta_h = 0$), both ends are compressed at the same time, so the plasma length oscillates while its center of mass remains fixed. In contrast, when $\theta_h = \pi$, the plasma length stays constant while its center of mass oscillates in z.

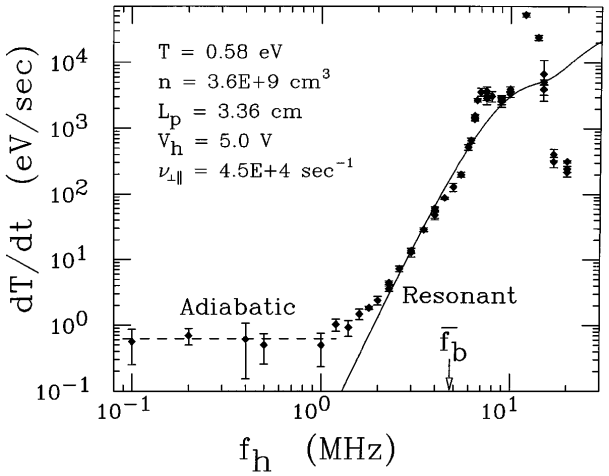

FIG. 2. Measured heating rates versus frequency of applied voltage. Adiabatic heating dominates at low f_h, while resonant heating dominates at high f_h (enhanced by damped-mode heating near 7 and 11 MHz). The dashed curve is from Eq. (1), and the solid curve is from Eq. (2), both with $\delta L/L_p = 0.0042$.

Figure 3 shows that low-frequency adiabatic heating is maximized when the end compressions are in phase, whereas higher frequency resonant heating is maximized when the compressions are out of phase. The squares show the measured heating rate for $f_h = 0.2$ MHz, where the maximum heating occurs for $\theta_h = 0$; at least 5 times less heating occurs for $\theta_h = \pi$. This is consistent with adiabatic heating, since the anisotropy between $T_\perp$ and $T_\parallel$ is proportional to the change in length of the plasma. The dashed curve shows the prediction of adiabatic theory, which is proportional to $\cos^2(\theta_h/2)$. Resonant heating is negligible here, since $f_h \ll \overline{f_b} = 2.5$ MHz.

The diamonds in Fig. 3 show the heating rate for $f_h = 2$ MHz $\sim \overline{f_b}$. Now the heating is smallest for $\theta_h = 0$ and 10 times larger for $\theta_h = \pi$. This is consistent with bounce resonance heating but not adiabatic heating. Let Δu be the change in the speed of an electron when it reflects from an oscillating sheath at the ends of the plasma. When $\theta_h = \pi$, an electron with bounce frequency $f_b = f_h$ (i.e., $\ell = 1$) receives identical Δu at each end of the plasma, causing a net change in the speed of the electron after one bounce orbit. In contrast, when $\theta_h = 0$, the Δu are of opposite sign at each end of the plasma, resulting in no net change in speed. That is, the Δu imparted by one oscillating sheath destructively interfere with the Δu imparted by the other.

However, the heating rate for $\theta_h = 0$ is over twice as large at $f_h = 2$ MHz as at 0.2 MHz. This is because only

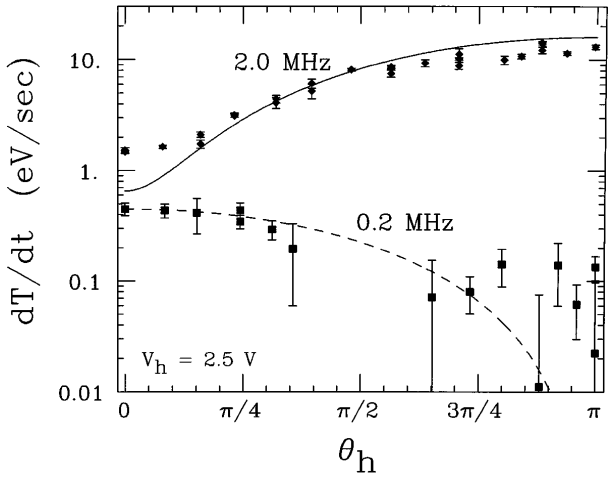

FIG. 3. Measured heating rates when both ends of the plasma are oscillated versus phase difference between the ends. Adiabatic (squares) and resonant (diamonds) heating rates have opposite dependence on θ_h. The dashed and solid curves show the predictions of the adiabatic and resonant theories, respectively, with $\delta L/L_p = 0.0022$. Here, $n = 2.1 \times 10^9$ cm^{-3}, $L_p = 4.86$ cm, $T = 0.31$ eV, and $\overline{f_b} = 2.5$ MHz.

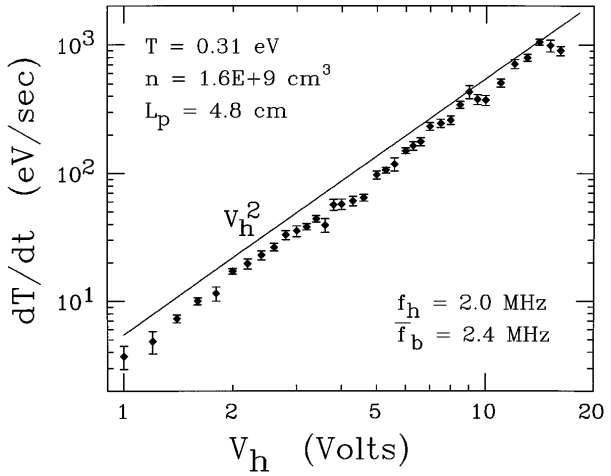

FIG. 4. Measured heating rate is proportional to the square of the amplitude of the applied voltage. The solid curve shows the prediction of Eq. (2) with $\delta L/L_p = 0.0024 V_h$.

the odd ℓ resonances suffer destructive interference for $\theta_h = 0$. The Δu received by electrons with $f_b = f_h/\ell$, $\ell = 2, 4, 6, \ldots$ *constructively* interfere at $\theta_h = 0$, giving a nonzero heating rate. These higher order resonances should cause less heating, because the resonant electrons are slower and encounter the oscillating sheaths less frequently; this agrees with our measurements.

Note that the dependence of dT/dt on θ_h is *not* due to the excitation of axial plasma modes, which would cause heating as they damp. A higher resolution frequency scan of the heating rate shows sharp peaks at $f_h \approx 7$ MHz and $f_h \approx 11$ MHz, each about 200 KHz wide and 10^5 eV/s high. While these modes cause the "steps" in the high f_h data in Fig. 2, the narrowness of the peaks and their occurrence only for $f_h > \overline{f_b}$ indicates that the heating for $f_h \leq \overline{f_b}$ is due to single particle resonances only.

The dependence of the resonant heating rates on the amplitude of the applied voltage V_h and on the plasma temperature T are shown in Figs. 4 and 5, respectively. The heating rate scales as V_h^2 over 2 orders of magnitude, and as $T^{-1/2}$ over 1 order of magnitude.

We compare our measurements to a bounce-resonance theory by Crooks and O'Neil [12]. The theory was originally developed to predict the radial electron flux in "rotational pumping" transport due to resonances between electron bounce and rotation frequencies. The prediction for the flux $\mathbf{\Gamma}$ [Eq. (98) in Ref. [12]] is converted to a heating rate prediction by using local conservation of energy, i.e., $-e\mathbf{\Gamma} \cdot \mathbf{E} = \frac{3}{2} n dT/dt$. Since the potential is uniform inside the plasma and abruptly decreases at the ends, the bounce length of an electron is independent of its energy. The applied voltage causes the position of the end sheath to oscillate as

$$z_{\text{end}}(t) = \delta L \sin(2\pi f_h t),$$

where $\delta L \ll L_p$. The magnetic field effectively confines the electrons in one-dimension between a fixed and a moving wall, just as in the Fermi acceleration model [13]. Each time an electron hits the moving wall, its speed changes by $\Delta u \equiv 2v_{\text{wall}} = 4\pi f_h \delta L \cos(2\pi f_h t)$. In the absence of collisions, Ref. [13] shows that for electrons with resonant bounce frequencies, $f_b \approx f_h/\ell$, the Δu add coherently, producing cyclical orbits in velocity space over multiple bounces. Heating arises due to the collisional exchange of energy between resonant and nonresonant electrons. Crooks and O'Neil calculate the heating rate in the "plateau" regime, where the resonant electrons travel only part way through a velocity-space cycle before colliding with another electron. In that case, the total change in speed of a resonant electron between

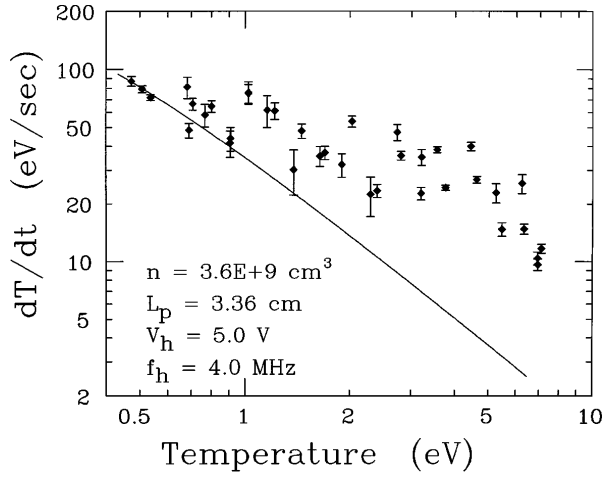

FIG. 5. Measured heating rate decreases slowly with plasma temperature. The solid curve shows the prediction of Eq. (2) with $\delta L/L_p = 0.0042$ and $\overline{f_b} = 6.22T(\text{eV})$ MHz.

collisions is

$$\Delta v \approx 4\pi f_h \delta L (f_b/\nu),$$

where ν is the rate at which electrons are knocked out of resonance due to collisions. The collisions give rise to velocity-space diffusion with step size Δv. This results in a velocity space flux of

$$\Gamma_v = -\nu(\Delta v)^2 \frac{\partial f}{\partial v},$$

where the $f(v,t)$ is the axial velocity distribution function. Linearizing f as $f(v,t) = f_0(v) + f_1(v,t)$, and using a velocity space continuity equation, $\partial f_1/\partial t + \partial \Gamma_v/\partial v = 0$, the heating rate is calculated from the flux by

$$\frac{\partial T}{\partial t} = \int \frac{1}{2} m_e v^2 \frac{\partial f_1}{\partial t} dv = -\int \frac{1}{2} m_e v^2 \frac{\partial \Gamma_v}{\partial v} = \int m_e v \Gamma_v \, dv .$$

Assuming that only resonant electrons contribute to the heating rate, the integral becomes a sum evaluated at speeds $v_\ell = 2 f_h L_p/\ell$. Performing this calculation rigorously, assuming f_0 is a Maxwellian and assuming a resonance width of $\delta v \approx \nu L_p/\ell\pi$, gives

$$\frac{dT}{dt} = \frac{(2\pi)^{3/2} f_h T}{3(L_p/\delta L)^2} \sum_{\ell=1}^{\infty} \left(\frac{f_h}{\ell \overline{f_b}}\right)^5 \exp\left[-\frac{1}{2}\left(\frac{f_h}{\ell \overline{f_b}}\right)^2\right]. \quad (2)$$

Note that the heating rate is independent of ν (hence the name plateau regime). When the two ends of the plasma oscillate with phase difference θ_h, the δL term in Eq. (2) changes to $2\delta L \sin(\theta_h/2)$ for odd ℓ and to $2\delta L \cos(\theta_h/2)$ for even ℓ.

Since all quantities in the theory are measurable, no adjustable parameters are needed to compare it with the data. We determine the amplitude δL of the wall oscillation from Eq. (1) by measuring the adiabatic heating rate dT/dt at low f_h. Both $\nu_{\perp\|}$ and adiabatic heating have been previously measured on our apparatus and shown to be in good agreement with theory. These measurements show that $\delta L \propto V_h$, and typically give $\delta L/L_p < 0.01$.

The predictions of Eq. (2) are shown as solid curves in Figs. 2 to 5. In Figs. 2 to 4, quantitative agreement within a factor of 2 is seen over a wide range of parameters and heating rates. Less accurate agreement is seen in Fig. 5, where the measured heating rates decrease more slowly with temperature than do the theoretical rates.

The reason for this discrepancy is not known. One possibility is that as T is increased, the collision rate decreases until the plasma is in the "banana" regime [14] rather than the plateau regime, so that Eq. (2) is not applicable. However, estimates of heating in the banana regime indicate that it is weaker than heating in the plateau regime, and decreases even faster with increasing temperature. This is the opposite of the observed behavior. Another possibility is that δL increases with temperature; however, numerical calculations indicate no such dependence.

Numerical work on Fermi acceleration predicts that electrons with $f_b < 2\pi(\delta L/L_p)^{1/2} f_h$ should move stochastically through velocity space [13], which violates the assumption of Crooks and O'Neil of discrete resonant electron orbits. However, stochasticity should simply increase the rate at which electrons enter and leave resonance, thus increasing the effective collision rate ν. Since the heating rate is independent of ν, Eq. (2) should still be valid in the stochastic regime [15]. This is verified experimentally by the highest V_h data in Fig. 4, where $\delta L/L_p = 0.038$.

The close agreement between data and theory suggests that resonant particle rotational pumping [12] should be observable in the proper regime. Furthermore, it suggests that asymmetry-induced transport in non-neutral plasmas [16] may have a resonant particle component despite the current lack of experimental evidence. This is especially true in the case of asymmetries placed at the ends of a plasma column, such as the "rotating wall" [17].

The authors acknowledge fruitful and vigorous discussions with Eric Hollmann, Tom O'Neil, and Dan Dubin. This work was supported by National Science Foundation Grant No. PHY94-21318 and Office of Naval Research Foundation Grant No. N00014-96-1-0239.

*Present address: Los Alamos National Laboratory, Group P-24, MS-E526, Los Alamos, NM 87545.

[1] L. D. Landau, J. Phys. U.S.S.R. **10**, 25 (1946).
[2] J. H. Malmberg and C. B. Wharton, Phys. Rev. Lett. **13**, 184 (1964).
[3] M. Koepke *et al.*, Phys. Rev. Lett. **56**, 1256 (1986).
[4] H. Hojo and T. Hatori, J. Phys. Soc. Jpn. **62**, 2212 (1993).
[5] K. C. Shaing and A. Y. Aydemir, Phys. Plasmas **4**, 3163 (1997).
[6] N. I. Grishanov, C. A. de Azevedo, and A. S. de Assis, J. Geophys. Res. **101**, 7881 (1996).
[7] H. Karimabadi, D. Krauss-Varban, and T. Terasawa, J. Geophys. Res. **97**, 13 853 (1992).
[8] C. S. Weimer *et al.*, Phys. Rev. A **49**, 3842 (1994).
[9] G. Dimonte, Phys. Rev. Lett. **60**, 1390 (1988).
[10] C. F. Driscoll, K. S. Fine, and J. H. Malmberg, Phys. Fluids **29**, 2015 (1986); D. L. Eggleston, Phys. Plasmas **4**, 1196 (1997).
[11] B. R. Beck, J. Fajans, and J. H. Malmberg, Phys. Plasmas **3**, 1250 (1996).
[12] S. Crooks and T. M. O'Neil, Phys. Plasmas **2**, 355 (1994).
[13] M. A. Lieberman and A. J. Lichtenberg, Phys. Rev. A **5**, 1852 (1972).
[14] A. A. Galeev and R. Z. Sagdeev, Sov. Phys. JETP **26**, 233 (1968).
[15] T. M. O'Neil (private communication).
[16] J. Notte and J. Fajans, Phys. Plasmas **5**, 1123 (1994).
[17] X.-P. Huang *et al.*, Phys. Rev. Lett. **78**, 875 (1997).